Design of a Single-Fiber, Wavelength-Resolved System for Monitoring Deep Tissue Oxygenation

Linhui Yu and Kartikeya Murari

Abstract— **We propose a single-fiber, zero source-detector separation system with wavelength-resolved detection for measuring oxygen saturation in deep brain structures. The system consists of a white light emitting diode (LED) source, optics to couple light into a 240-μm-diameter fiber, a beam splitter to separate the collected from the delivered photons and a spectrometer for detection. Depth resolution is achieved by inserting the fiber, comparable in size to microelectrodes used for electrophysiology, into the tissue of interest. Since most of the diffuse reflected light travels through a small volume at the tip of the fiber, this arrangement allows efficient collection of signal. Fresnel reflections are minimized using polarizers. Monte Carlo simulations across 400-1000 nm indicate that $\sim$0.5% of the incident light can be collected and effectively interrogate a $\sim$0.02 mm^3 volume at the fiber tip. System design, characterization data and phantom experiments using an absorptive dye in scattering media are presented. The simple nature of the instrumentation can potentially lead to a miniaturized system capable of detecting oxygen saturation in deep brain structures in freely-moving animals.**

I. INTRODUCTION

Near infrared spectroscopy (NIRS) is widely used to quantify the absolute concentration of chromophores in tissue. Wavelengths between 700 nm and 1000 nm are generally used, in which scattering is much stronger than absorption, thus light can penetrate deeper into tissue. The dominant chromophores absorbing light in the NIR band are oxyhemoglobin (HbO), deoxyhemoglobin (Hb) and water. The attenuation spectra from back reflected or transmitted light are detected, and are related to the changes to different chromophores using the modified Beer Lambert law. Oxygen saturation, as a sign of activity, can be determined according to the different concentration of hemoglobin [1], [2].

In typical NIRS systems, illumination and detection is at the surface of the tissue being imaged while the region of interest is deeper. Since there is a very large non-specific reflection from the surface and the superficial part of the tissue, two schemes have been developed to obtain sub-surface information. One uses a pair of probes, one acting as a light source and the other as a detector, with a certain source-detector separation and wavelength-resolved detection [3]. The separation allows the collection of photons that have travelled deep in the tissue, permitting sub-surface measurements. However, very few photons can be collected, requiring high-power sources and high-sensitivity detectors. Another technique that works with zero source-detector separation uses ultra-high-speed sources and detectors to temporally discriminate among photons returning from different depths in the tissue [4]. In such systems, sources and detectors are usually fiber-coupled to benchtop components. Due to the sensitivity or speed of the components required, the depth resolution comes at an expense of increased system size and complexity. Specifically, when monitoring oxygen saturation in the brain for neuroscience studies, such systems are typically used with anaesthetised animals. This leads to biased results because anesthesia suppresses normal physiology.

Here, we propose a system using a single fiber for both light delivery and collection with a zero source-detector separation. We focus on the design of the optical system to acquire the backscattered spectrum, which can then be related to oxygen saturation using existing algorithms [2]. A free-space source is used to couple light into the fiber and a beam splitter is used to separate the excitation and collection light. The depth resolution of the system arises from the fact that the fiber is implanted deep within the brain rather than illuminating the surface. The system is designed to interrogate a small volume of tissue near the tip of the fiber. The 240-μm-diameter fiber used is comparable in size to metal microelectrodes used for stimulation and recording and is not expected to cause substantial tissue damage. The zero source-detection separation ensures many photons are collected, relaxing power and sensitivity requirements for the source and detector. Since the bulk of the detected photons, apart from the Fresnel reflections at the air-fiber and fiber-tissue interface, have travelled through a small volume near the fiber tip, no specialized discrimination is needed. A compact polarization-based scheme was used to minimize the effects of reflection at the air-fiber interface.

Section II of the paper discusses the optical design of the system and section III describes a series of Monte Carlo simulations used to model the system. Section IV presents characterization results and data from preliminary phantom experiments and section V discusses further work and concludes the paper.

II. SYSTEM DESIGN

Figure 1 shows a schematic drawing and a photograph of the proposed system. Briefly, light from an LED is collimated, polarized, focused and coupled into a fiber. The fiber delivers light into the sample and collects a portion of the backscattered light. A beam splitter in the collimated beam path separates this signal from the excitation and

This work was supported by the Department of Electrical and Computer Engineering, NSERC and CMC.

Linhui Yu linhyu@ucalgary.ca and Kartikeya Murari kmurari@ucalgary.ca are with the Department of Electrical and Computer Engineering, University of Calgary, Calgary, AB T2N 1N4, Canada.

978-1-4244-7929-0/14/$26.00 ©2014 IEEE

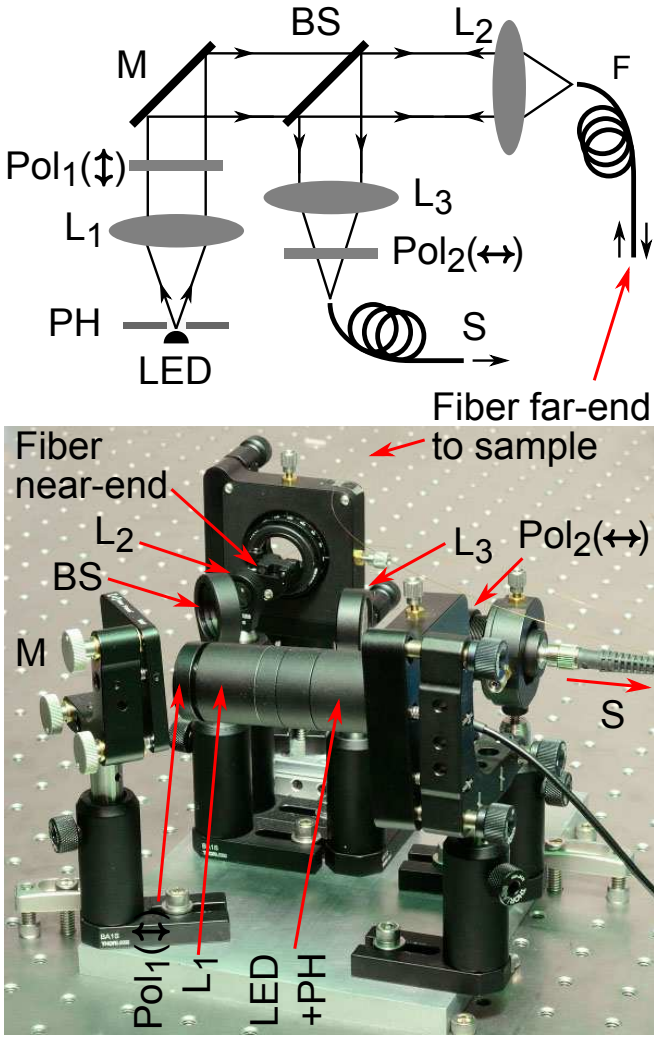

Fig. 1. Schematic drawing and photograph of the system showing light emitting diode (LED), pinhole (PH), collimating lens (L_1), mirror (M), beam splitter (BS), focusing lenses (L_2, L_3), fiber (F), polarizers (Pol_1, Pol_2) and spectrometer (S).

directs it, through a second crossed polarizer to attenuate Fresnel reflection, towards a spectrometer for analysis.

A. Light Source and Fiber Coupling

A phosphor-based white LED (C503D-WAN, Cree, NC), covering a wavelength band from 425-675 nm, was used as the light source. In order to efficiently collimate the light, the LED lens was removed and the surface was polished such that a 600 μm aperture could be put as close as possible to the emitting area on the semiconductor die. This source was then imaged into a 200-μm-core, 240-μm-diameter, 0.22 numerical aperture (NA) fiber (UM22-200, Thorlabs, NJ). This needs a 3:1 focal length ratio between the collimating and focusing lenses. In addition, the NA of the fiber enforces a lower limit on the focal length of the focusing lens. The system was modelled using Zemax (Zemax, WA) and we chose 60 mm and 19 mm lenses (AC127-019-A, AC254-060-A, Thorlabs, NJ) which predicted a sub-200-μm diameter spot. The system was constructed using kinematic mounts for the LED and a steering mirror, and a 5-axis mount to hold the fiber. The fiber delivers light to the sample and also collects a portion of the backscattered light.

B. Beam Splitter

A 50:50 beam splitter (EBP1, Thorlabs, NJ) was introduced in the collimated lightpath to separate the light returning through the fiber from the excitation. This light consists of the collected backscattered light from the sample, which constitutes our signal, and Fresnel reflections from both the near-end air-fiber and far-end fiber-sample interfaces, which form an undesirable background. The beam splitter directs half of this light towards the detector. The beam splitter also halves the light being coupled into the fiber. Both these losses are trade-offs imposed due to the usage of a single fiber.

C. Polarizers

Of the Fresnel reflections at the two interfaces mentioned above, reflections from the near-end coupling interface are more severe due to a large refractive index mismatch and proximity to the detector. This can overwhelm the small signals expected. To reduce this, a polarizer (LPVISE2X2, Thorlabs, NJ) was used to polarize the LED light along the vertical axis (Fig. 1: Pol_1). Fresnel reflections at the near-end air-fiber interface maintain vertical polarization and are excluded from the detector by a second horizontal polarizer (Fig. 1: Pol_2). The fiber randomizes polarization of the backscattered light that travels through it, and while this is also attenuated by Pol_2, the degree of attenuation is much smaller than that for the vertically polarized background. In effect, the polarizers increase the signal to background ratio while reducing the signal strength. This can be compensated by stronger excitation or a more sensitive detector.

D. Detector

The collected light was analysed using a non-scanning, charge coupled device based spectrometer (Maya 2000 Pro, Ocean Optics, FL). The instrument has a range of 165-1100 nm and a nominal resolution of $\sim$0.4 nm/pixel.

III. MONTE CARLO SIMULATIONS

Typical NIRS system uses continuous wave light source and measures transmitted spectrum with different source-detector separation. In our system, we use the same fiber to deliver and collect light, so there is no source-detector separation. Spatial resolution comes from the fact that the bulk of the light being collected by the fiber travels through a small volume at the fiber tip. Two simulations using the Monte Carlo program for multi-layered media [5] were performed to estimate this. For the simulations, the scattering coefficient and anisotropy coefficient of the Mie theory approximation of 10% intralipid were used [6]. Tissue absorption was approximated as 150 g/L hemoglobin in a mixture of 90% water and 10% soybean oil [7] and the refractive index was set to 1.37. In each simulation, 10^6 photons were injected into the tissue, and the results convolved [8] to obtain the response for a 200-μm-diameter uniform profile beam.

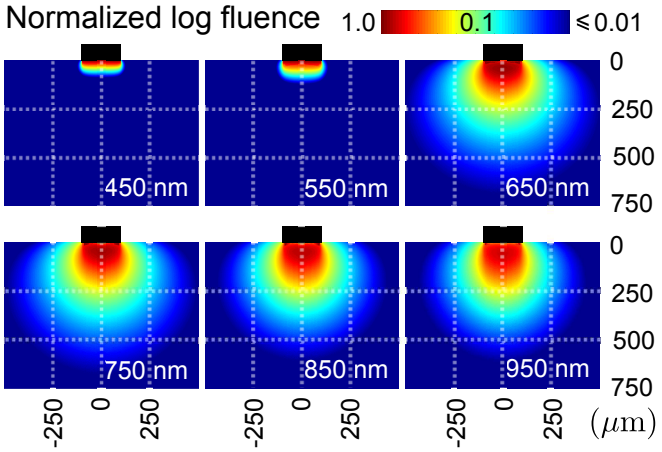

Fig. 2. Normalized log fluence as a function of radial and axial distance at six wavelengths. The black bar indicates the 200 μm fiber core

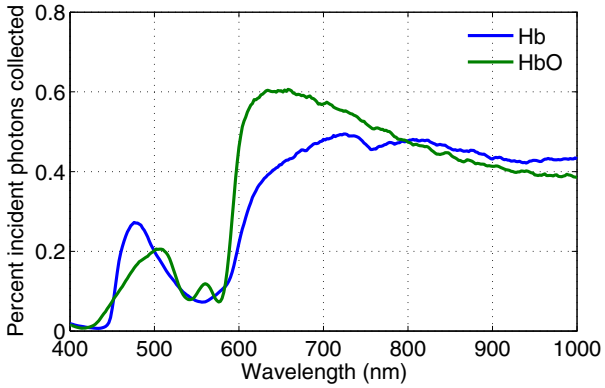

Fig. 3. Percent incident photons collected by the 200-μm-core, 0.22 NA fiber for oxygenated and deoxygenated blood

The first simulation was done to visualise the penetration of light into the tissue. Figure 2 shows the normalized log fluence as a function of radial and axial distance at six wavelengths ranging from 450 to 950 nm. This simulation assumed that hemoglobin is 100% oxygenated. The data indicates that the penetration of photons into tissue is confined to relatively small volumes at all wavelengths simulated. Using the simulations, it was calculated that outside a volume that varied from 0.002 mm^3 at 450 nm to 0.021 mm^3 at 950 nm, the fluence drops to under 10% of the peak. A subset of the photons from this volume would diffuse back towards the fiber and be collected giving the system its spatial resolution.

The next simulation was performed to estimate what percentage of photons would undergo diffuse reflection and be collected by the fiber given its diameter and numerical aperture (NA). Figure 3 shows the percentage of incident photons collected by the fiber for the wavelengths between 400 and 1000 nm. The simulation was run every 2 nm with the same settings as described above. The diffuse reflectance was calculated as a function of radial distance and exit angle. Photons exiting within a 100-μm-radius and at angles less than or equal to that corresponding to the fiber NA of 0.22 were assumed to be collected and summed to estimate the percentage of incident light collected. The results show that even with a small-diameter fiber, a measurable signal, which is modulated based on hemoglobin oxygenation, can potentially be detected. While the collected signal is stronger in the red-NIR band, the spectra show more peaks and valleys in the blue-red region, which might make separating the contributions easier. The signal strength, less than typical Fresnel reflections, underscores the requirement to minimize any background signal.

IV. RESULTS

A. Characterization

To align the system, a power meter was used to iteratively maximize the light intensity at the far-end of the fiber and at the location of the detector. Since broadband light was used, absolute power measurement are not useful, however relative measurements can still be interpreted. The size of the focused light spot was tested using a pinhole. About 91% of the light passed through the 200-μm-diameter pinhole used. The fiber coupling efficiency was $\sim$70%. This was somewhat lower than expected from the Zemax simulations and likely due to NA mismatches. The focusing lens NA was about 0.2 for all wavelengths and while the fiber NA was specified at 0.22$\pm$0.02, its wavelength variation was not known.

As mentioned earlier, we expected the polarizers to attenuate both the signal and the background, but increase the signal to background ratio. To test this, we measured ratios of power received at the detector with and without the polarizers. Two measurements were done, one with the far-end of the fiber in air and one with the far-end immersed in glycerine. In the former, Fresnel reflections from the far-end fiber-air interface constitute the signal. In the latter, due to matched indices, there is no signal from the far-end. In both cases, Fresnel reflections from the near-end fiber-air interface constitute the background. With the two polarizers, signal plus background was reduced by a factor of $\sim$12, indicative of the $\sim$40% random-polarized-light transmission of the polarizers. At the same time, the background was reduced by a factor of $\sim$130, indicating a ten-fold improvement in the signal-to-background ratio. To further characterize this, and to test wavelength discrimination, we used a red paper facing the far-end of the fiber to reflect some of the incident light back into the fiber and analysed the data with and without polarizers. The results are shown in Fig. 4. The dashed lines in the upper plot show the spectra received with the fiber tip in air with and without polarizers and are due to background from both ends of the fiber. These spectra were unexpectedly different because the white LED was not randomly polarized across its entire range. All spectra were normalized using the blue peak in these spectra. Received spectra with the red paper in front of the fiber are shown in solid lines and are stronger as they include some backscattered signal in addition to the background. As expected, this increase is more dominant in the red region. The lower plot shows the ratio of the signal and background to the background alone, and clear improvements can be seen. The improvement is less

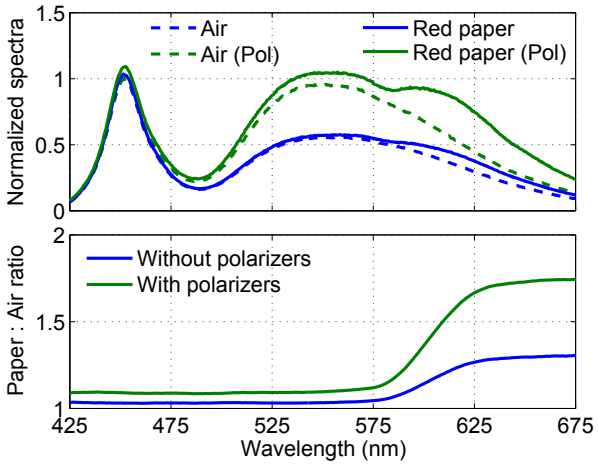

Fig. 4. Normalized detected spectra with fiber tip in air and facing a red paper with and without polarizers (top) and ratio of the detected spectra (bottom) showing the improvement in the signal to background ratio.

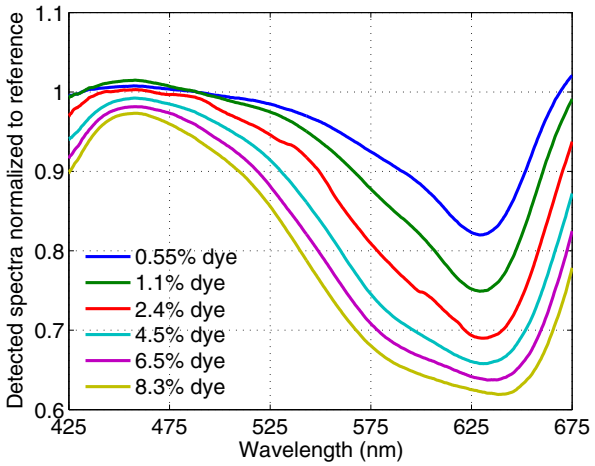

Fig. 5. Detected spectra normalized to a reference spectrum for different absorptions in the scattering phantom controlled by varying the concentration of an absorptive dye in the phantom.

than the 10-fold prediction, likely due to residual background from the far-end fiber-air interface, which was removed using index matching in the previous test, and the non-random polarization of the LED, which was not accounted for. All spectra were smoothed using a 20-nm sliding window.

B. Experimental Data

To test the operation of the system in a tissue phantom, we used a test solution with 10% vol./vol. lipid emulsion in water to account for scattering and added a water-based dye to change the absorption. In order to avoid diluting the lipid emulsion with the water base of the dye, a pre-calculated amount of the lipid was added to the solution along with the dye each time. Thus, we expected the scattering to remain constant while the absorption changed. First, the far-end of the fiber was immersed in the phantom and the reference reflection spectrum was recorded. Then, measured quantities of the dye/lipid solution were added gradually to change the concentration of dye. A magnetic stirrer was used to ensure homogeneity. The collected spectra with different dye concentrations were recorded and their ratio to the reference spectrum is shown in Fig. 5. From the results we can see that the reflection reduces as the concentration of dye increases. Since the concentration of the lipid emulsion stays the same, the scattering effect is identical in each test, but as the concentration of the dye increases, the absorption increases and the amount of reflection decreases. All spectra were smoothed using a 20-nm sliding window.

V. Conclusions and Discussion

We have built a single-fiber, zero source-detector separation system, that when combined with appropriate processing algorithms, can monitor oxygen saturation by analysing the spectrum of light backscattered from tissue. Monte Carlo simulations show that photons collected by the fiber mainly represent the property of tissue within a $\sim$0.02 mm^3 volume near the fiber tip and that $\sim$0.5% of the incident photons could be collected using a 200-μm-core, 0.22 NA fiber. Preliminary experimental results in a scattering tissue phantom indicated that the system is sensitive to absorption changes.

Potential improvements in the system include using a higher NA fiber and a microlens at the fiber tip to increase collection; anti-reflection coatings, polarization sensitive beam splitters or an all-fiber/GRIN lens approach to minimize back reflections; and a relatively narrower band light source optimized according to the simulations. The system can be potentially miniaturized by butt-coupling the LED to a fiber, using GRIN-lens-based collimation and focusing, and a cube beamsplitter coupled to an integrated spectrometer. While challenging, this will allow oxygen saturation to be monitored in deep brain structures with no fiberoptic or electrical tethers in freely-moving animals, that will allow long-term studies in a close-to-natural environment.

References

[1] D. Delpy and M. Cope, "Quantification in tissue near–infrared spectroscopy," *Philosophical Transactions of the Royal Society of London. Series B: Biological Sciences*, vol. 352, no. 1354, pp. 649–659, 1997.

[2] T. Vo-Dinh, *Biomedical Photonics Handbook*. CRC press, 2010.

[3] T. Durduran, R. Choe, W. Baker, and A. Yodh, "Diffuse optics for tissue monitoring and tomography," *Reports on Progress in Physics*, vol. 73, no. 7, p. 076701, 2010.

[4] M. Mazurenka, A. Jelzow, H. Wabnitz, D. Contini, L. Spinelli, A. Pifferi, R. Cubeddu, and A. D. Mora, "Non-contact time-resolved diffuse reflectance imaging at null source-detector separation," *Optics Express*, vol. 20, no. 1, pp. 283–290, 2012.

[5] L. Wang, S. L. Jacques, and L. Zheng, "MCML - Monte Carlo modeling of light transport in multi-layered tissues," *Computer Methods and Programs in Biomedicine*, vol. 47, no. 2, pp. 131–146, 1995.

[6] H. J. Van Staveren, C. J. Moes, J. van Marie, S. A. Prahl, and M. J. Van Gemert, "Light scattering in intralipid-10% in the wavelength range of 400-1100 nm," *Applied Optics*, vol. 30, no. 31, pp. 4507–4514, 1991.

[7] S. T. Flock, S. L. Jacques, B. C. Wilson, W. M. Star, and M. J. van Gemert, "Optical properties of intralipid: a phantom medium for light propagation studies," *Lasers in Surgery and Medicine*, vol. 12, no. 5, pp. 510–519, 1992.

[8] L. Wang, S. L. Jacques, and L. Zheng, "CONV - convolution for responses to a finite diameter photon beam incident on multi-layered tissues," *Computer Methods and Programs in Biomedicine*, vol. 54, no. 3, pp. 141–150, 1997.